Geant4-DNA simulation of human cancer cells irradiation with helium ion beams

Konstantinos Chatzipapas, Milos Dordevic, Sara Zivkovic, Ngoc Hoang Tran, Nathanael Lampe, Dousatsu Sakata, Ivan Petrovic, Aleksandra Ristic-Fira, Wook-Geun Shin, Sara Zein, et al.

Geant4-DNA simulation of human cancer cells irradiation with helium ion beams

Konstantinos Chatzipapas[1], Milos Dordevic[2], Sara Zivkovic[2], Ngoc Hoang Tran[1], Nathanael Lampe[3], Dousatsu Sakata[4], Ivan Petrovic[2], Aleksandra Ristic-Fira[2], Wook-Geun Shin[5], Sara Zein[1], Jeremy M.C. Brown[6], Ioanna Kyriakou[7], Dimitris Emfietzoglou[7], Susanna Guatelli[8], Sebastien Incerti[1]

[1]University of Bordeaux, CNRS, LP2i, UMR5797, F-33170 Gradignan, France

[2]Vinca Institute of Nuclear Sciences, National Institute of the Republic of Serbia, University of Belgrade, Mike Petrovica Alasa 12-14, 11351 Vinca, Belgrade, Serbia

[3]Independent researcher, Melbourne, Australia

[4]Division of Health Sciences, Osaka University, Osaka 565-0871, Japan

[5]Physics Division, Department of Radiation Oncology, Massachusetts General Hospital and Harvard Medical School, Boston, 02114 MA, USA

[6]Optical Sciences Centre, Department of Physics and Astronomy, Swinburne University of Technology, Hawthorn 3122, Australia

[7]Medical Physics Laboratory, Department of Medicine, University of Ioannina, 45110 Ioannina, Greece

[8]Centre for Medical Radiation Physics, University of Wollongong, Wollongong, NSW 2522, Australia

(Dated: June 26, 2023)

Abstract

Purpose: This study aimed to develop a computational environment for the accurate simulation of human cancer cell irradiation using Geant4-DNA. New cell geometrical models were developed and irradiated by alpha particle beams to induce DNA damage. The proposed approach may help further investigation of the benefits of external alpha irradiation therapy.

Methods: The Geant4-DNA Monte Carlo (MC) toolkit allows the simulation of cancer cell geometries that can be combined with accurate modelling of physical, physicochemical and chemical stages of liquid water irradiation, including radiolytic processes. Geant4-DNA is used to calculate direct and non-direct DNA damage yields, such as single and double strand breaks, produced by the deposition of energy or by the interaction of DNA with free radicals.

Results: In this study, the "molecularDNA" example application of Geant4-DNA was used to quantify early DNA damage in human cancer cells upon irradiation with alpha particle beams, as a function of linear energy transfer (LET). The MC simulation results are compared to experimental data, as well as previously published simulation data. The simulation results agree well with the experimental data on DSB yields in the lower LET range, while the experimental data on DSB yields are lower than the results obtained with the "molecularDNA" example in the higher LET range.

Conclusion: This study explored and demonstrated the possibilities of the Geant4-DNA toolkit together with the "molecularDNA" example to simulate the helium beam irradiation of cancer cell lines, to quantify the early DNA damage, or even the following DNA damage response.

Keywords: Geant4-DNA, molecularDNA, simulation, cancer, helium, irradiation

I. INTRODUCTION

In contemporary cancer treatment, there is an increased use of facilities providing beams of protons and carbon ions, given their advantage over gamma ray irradiation (Petrovic *et al.*[1,2]). Such radiation therapy has the primary effect of causing different types of DNA damage, including single and double strand breaks, DNA-base damage and DNA-protein cross links. From the radiobiological point of view, an essential cellular event is the double strand break (DSB), which is considered to be a dangerous type of lesion, more difficult to repair by cellular mechanisms than the single strand breaks (SSB), as detailed in Cannan *et al.*[3]. DSB could lead to chromosome aberrations, which may later lead to cancer or cell death, as shown in Chatzipapas *et al.*[4], 2020.

As described in Kramer *et al.*[5], there is a focus on the investigation of possibilities to use alpha particle beams to kill malignant cells. It is known, based on previous radiobiological studies, that the relative biological effectiveness (RBE) of alpha particle beams is higher than the RBE of protons and lower than that of carbon ions, as shown in Loeffler *et al.*[6]. Treating with helium ion beams, i.e. alpha particles, certain types of tumours and specific situations, like deep seated and paediatric tumours, may be more beneficial compared to other irradiation methods. Alpha particle beams have intermediate properties and could fill the gap between the use of proton and carbon beams. More specifically, helium ion beams cause less projectile fragmentation than carbon ions, having substantially shorter fragmentation tail. Additionally, they have less lateral beam spread, a reduced energy and path length straggling and scattering than proton beams, as shown in Mein *et al.*[7]. Moreover, a helium-beam cancer treatment facility would offer a significant reduction in cost and size in comparison with carbon ions treatment facility, as shown in Sapinski *et al.*[8]. The use of alpha particles could represent a promising compromise between proton therapy, which in theory is less efficient than helium ion therapy from the biological point of view, and carbon therapy for which secondary particles in the tail of the Bragg curve are problematic, as described in Tinganelli *et al.*[9]. Early clinical trials with therapeutic alpha particle beams carried out between 1977 and 1993 at Lawrence Berkeley National Laboratory (LBNL) have successfully treated 2000 patients (Mein *et al.*[7], Ebner *et al.*[10]). Further preclinical studies with alpha particle beams that took place at the Heidelberg Ion-Beam Therapy Center (HIT) (Norbury *et al.*[11], Mairani *et al.*[12] and Tessonnier *et al.*[13]) underlined the importance

of further understanding the radio-biological parameters that are relevant to alpha particle beams.

The scarcity of experimental data on irradiations by helium ion beams is a limiting factor for an accurate validation of Monte Carlo simulations of human cell irradiations with such beams. Several studies exist in the literature on Monte Carlo simulation of alpha particle irradiation at the cellular level. Among them, in 1995, Monte Carlo studies of DNA damage induced by protons and alpha particles at various values of the LET (Ottolenghi *et al.*[14], 1995) were performed using the MOCA-15 track structure code (Paretzke *et al.*[15], 1987). The SSB, DSB and deletions (complex lesions which involve at least two DSB within a small number of base pairs) were calculated in a wide range of LET from 10 $keV/\mu m$ to 220 $keV/\mu m$. In 2006, a comparison of three cellular irradiation techniques with alpha particles was performed using the Geant4 toolkit for an electrodeposited source of alpha particle emitting radionuclides, for irradiation with a random classical alpha beam and for a focused alpha microbeam line dedicated to single cell targeted irradiation (Incerti *et al.*[16], 2006). This allowed for the calculation of the distribution of hits among the population of cells and the absorbed dose for two typical cell geometries. Results of the simulation showed a strong dependence of the absorbed dose distribution with the cell geometry. In 2009, a dosimetry calculation at the single-cell level was performed for the microbeam irradiation facility at CENBG using the Geant4 simulation toolkit (Incerti *et al.*[17], 2009). The geometry model was based on high-resolution three-dimensional voxelised phantoms of human (HaCaT) cells, obtained from the combination of confocal microscopy imaging and ion beam chemical elemental analysis. Results were produced for single-cell irradiation using 3 MeV incident alpha particles. In 2012, this study was further expanded to utilize realistic cell nuclei geometries in Monte Carlo simulations and to consider a variety of different geometries encountered in a realistic population of cells (Barberet *et al.*[18], 2012). Inside the nuclei, the energy deposition patterns were simulated and the results compared with DNA damage measured using immuno-staining experiments. In the same year, Geant4-based Monte Carlo simulation was developed to model tumor antivascular alpha therapy (TAVAT) from the microdosimetry point of view (Huang *et al.*[19], 2012). The spatial non-uniform distribution of the alpha particles emitted from a ^{213}Bi source was simulated using the Geant4 toolkit. The obtained results were applied to interpret the clinical trial. Cell survival rate and therapeutic gain were determined. The results showed that tumor antivascular alpha therapy has the

potential to deliver a lethal dose to the tumor capillary endothelial cells, with an acceptable toxicity profile imposed on the normal surrounding tissue. In 2020, a study of mixed beam of high- and low-linear energy transfer was performed (Brzozowska *et al.*[20], 2020). This study was based on the assumption that the biological effect achieved is equal to the sum of effects of the individual (mixed) beam components. The mixed beam was composed of alpha particles and X-rays. The simulation was performed using the PARTRAC (Friedland *et al.*[21], 2003) Monte Carlo code for DNA damage calculation. The level of synergy depended on the mixed beam composition, with the highest level achieved at the 50:50 ratio of alpha particles and X-rays. In 2019, the energy spectrum of a LINAC was simulated for DNA molecules irradiation (Chatizipapas *et al.*[22], 2019) using the Geant4-DNA toolkit. In 2021, a novel computational platform referred to as IDDRRA (DNA Damage Response to Ionizing RAdiation) based on Geant4-DNA toolkit was proposed to study radiation induced DNA damage (Chatizipapas *et al.*[23], 2021). In 2021, results on DSB yields for alpha particles, published in Shin *et al.*[24] were performed using a private and older version of Geant4-DNA and a prototype version of the "molecularDNA" example application, showing consistency with the experimental data from Hoglund *et al.*[25]. However, the experimental data from Hoglund *et al.*[25] was limited to only one irradiation point, with a LET value of 40 $keV/\mu m$, thus being unable to validate the slightly decreased DSB yield for alpha particles as a function of LET that is reported in the simulation study of Shin *et al.*[24]. Simulations of DNA damage induced by proton and alpha particle beams in three different human cell nuclei geometries representing fibroblasts, lymphocites and endothelial cells were also performed using a simulation chain[26] based on Geant4-DNA and described in Tang *et al.*[27]. The irradiation of each of the three cell nucleus models was simulated for alpha particles with a LET value of 32.65, 84.68 and 212.50 $keV/\mu m$ and compared with experimental data from Frankenberg *et al.*[28]. The simulation results are in a good agreement with experimental data for LET below 50 $keV/\mu m$, while for higher LET values the experimental data points are lower than simulated. This was due to the fact that, as explained in[28], the loss of experimentally observable DNA fragments is higher than the DSB increase at LET higher than 50 $keV/\mu m$.

A new Geant4-DNA example application named "molecularDNA" was publicly released in December 2022 in the 11.1 version of Geant4, as described in Chatzipapas *et al.*[29], 2023. This example includes a geometrical model of a human cell, consisting of a continuous

Hilbert curve that produces a fractal-based DNA chain, which is made of straight and turned chromatin sections including nucleosomes. This DNA chain is placed inside an ellipsoid that imitates the human cell nucleus. The "molecularDNA" example enables the simulation of the physical, physico-chemical and chemical stages following the particle irradiation of the pre-defined human cell geometries. The example enables the calculation of the direct and non-direct early DNA damage and a quantitative measure of this damage through counting the induced number of single strand breaks (SSB), DSB, as well as the DNA fragments distribution. These biological endpoints calculated using the "molecularDNA" application could facilitate a comparison of simulation results with experimental or real-life data, providing also more information about the overall impact of each irradiation stage. The design of a human cell or bacterial geometries could enable the investigation of radiation impact on a particular system or environment, such as prolonged exposure to radionuclides, or in research related to extraterrestrial life in our solar system. The application is suited for novice users and can be utilized following simple macro commands. It is foreseen to include new cell geometries in the near future and incorporate new models to enable interactions in media other than water, and also to study more complex systems such as assemblies of cells, multicellular organisms or tissues.

In this study, two characteristic cancer cell lines, the lung carcinoma HTB-177 and breast adenocarcinoma MCF-7, were modelled and incorporated into the "molecularDNA" example, starting from the default "human cell" geometry already available in the example. The realistic cell geometry was obtained through available morphometric experimental data[30]. The simulation of the irradiation of these two cell lines with alpha particle beams was performed in the targeted LET range up to 80.3 keV/μm, allowing the comparison with experimental data from alpha particle irradiation[30], as well as with *in-silico* data from the literature. In order to provide an accurate comparison of collected data from alpha particle irradiation (Ristic-Fira *et al.*[30], 2023), the same experimental conditions, which are previously described in detail for the determination of DNA damage yield in the case of proton and carbon ion irradiations, are now strictly respected in all experimental campaigns with helium ions (Keta *et al.*[31], 2021).

II. MATERIALS AND METHODS

A. Human cancer cell geometry in "molecularDNA"

In the "molecularDNA" example of Geant4, the "human cell" geometry is implemented as a continuous Hilbert curve, which produces a fractal-based DNA chain structure approximately 6.4 Gbp long[32], placed inside an ellipsoid with semi-axes of $7.1\mu m \times 2.5\mu m \times 7.1\mu m$. In this setup, the effective DNA density in the nucleus is $\sim 0.015\ bp/nm^3$. The fractal-based geometry was initially developed by Lampe *et al.*[33–35] using the FractalDNA tool[36]. The radiation-induced DNA damage modelling was further developed and described by Sakata, Shin *et al.*[24,37–41]. Other important Geant4-DNA studies were made recently, such as simulations of water radiolysis in the presence of scavengers published in Chappuis *et al.*[42], offering perspective for more realistic modeling and improved understanding of biological systems response to radiation. The Geant4-DNA package was also used to simulate radiation transport in micro- and nanodosimeters, used in radiation protection, that are physically operated with tissue-equivalent gases such as nitrogen and propane, extending correspondingly the cross section data available in Geant4-DNA, as shown in the studies of Pietrzak *et al.*[43]. An example of human cell geometry, presenting cytoplasm, cell nucleus structure and alpha particle source is shown in Figure 1.

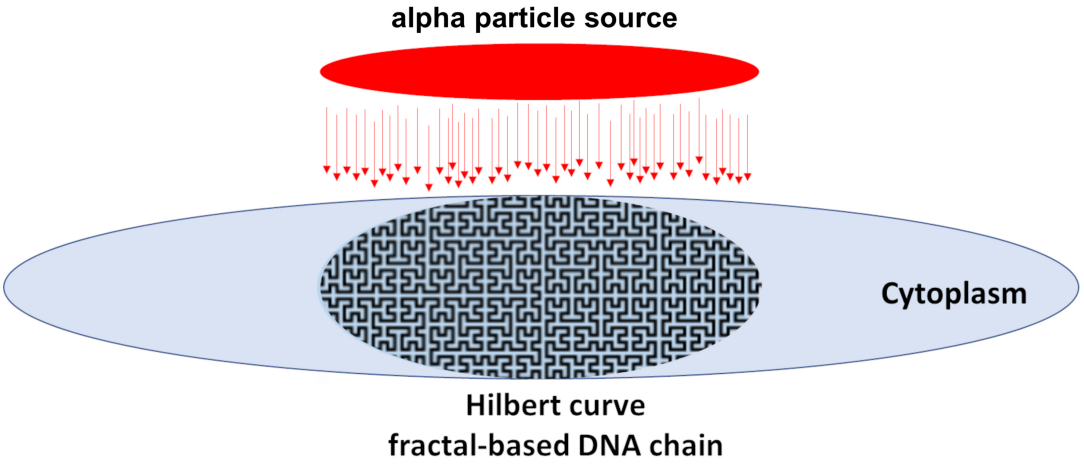

FIG. 1: A schematic illustration of human cell geometry and source, implemented in the "molecularDNA" Geant4 extended example[29]. Both the cytoplasm and the cell nucleus are considered to be made of liquid water. The cell is placed in vacuum.

B. Measurements of cancer cell geometries and dimensions

The HTB-177 (large cell lung carcinoma) and the MCF-7 (breast adenocarcinoma) human cells were collected from the American Tissue Culture Collection (ATCC), Rockville, MD, USA. These were grown as monolayers in RPMI-1640 medium, which was supplemented with 10% fetal bovine serum (FBS) and penicillin/streptomycin (Sigma-Aldrich Chemie GmbH, Steinheim, Germany). The cells were kept under standard conditions at 37°C in a humidified atmosphere with 5% CO_2 (Heraeus, Hanau, Germany). The average size of the cell nuclei for these two cell line studies was estimated by confocal microscopy using the ImageJ software[44]. The micrographic images of the two cell lines studied, magnified a hundred times, are shown in Figure 2. Cells were modelled to have an ellipsoidal shape and the corresponding semi-axes were measured as $8.55\pm0.41\ \mu m \times 2.50\pm0.25\ \mu m \times 6.43\pm0.30\ \mu m$ for the HTB-177 cell line and $7.01\pm0.33\ \mu m \times 2.50\pm0.25\ \mu m \times 5.30\pm0.26\ \mu m$ for the MCF-7 cell line. In comparison to the human cell dimensions used by default in "molecularDNA", as outlined in the previous subsection, HTB-177 cells have about 10% larger volume, while MCF-7 cell dimensions were measured to be $\sim 20\%$ smaller than the "molecularDNA" default cell geometry.

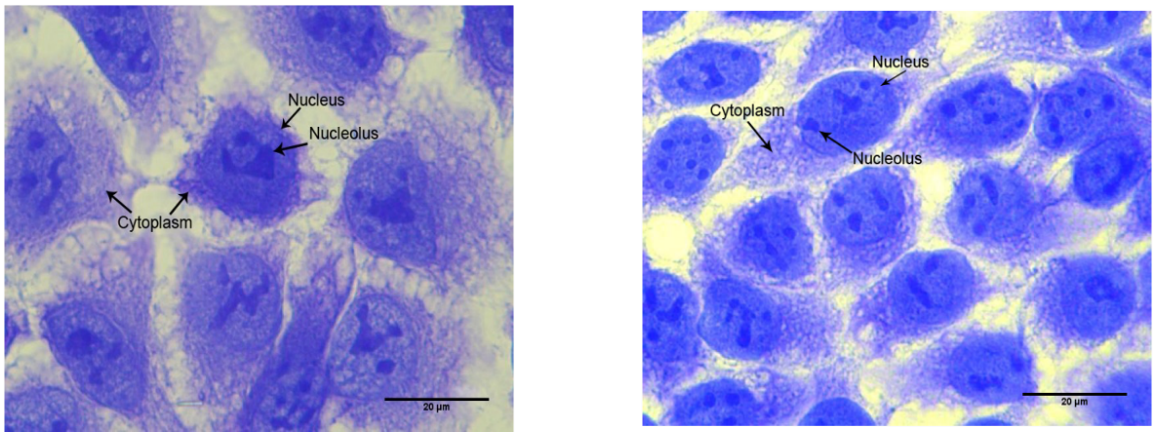

FIG. 2: Micrographs of HTB-177 (left) and MCF-7 (right) cells obtained using confocal microscopy.

C. Geometry modifications

Considering the difference in size for the different types of nucleus for HTB-177 and MCF-7 cell lines, with respect to the "molecularDNA" default values, as well as the fact

that a human cell has to include ∼6.4 Gbp of DNA[32], modified human cell geometries had to be developed. Within the scope of the "molecularDNA" example, there are ways to adjust such geometry by modifying the unit voxel size (each voxel has a cubical shape) and thus build such geometries, taking into account the number of nucleosomes. By applying subtle modifications to the voxel size and the number of nucleosomes, the value of ∼6.4 Gbp can be achieved essentially for any given cell dimensions, as illustrated in Figure 3. The far left picture presents the default case, available in "molecularDNA", with voxel size of 75 nm and 38 nucleosomes. Reducing the number of nucleosomes to 32 but keeping the voxel size constant at 75 nm results with the configuration shown in the middle left picture. If the number of nucleosomes is further reduced to 20, a configuration such as the one presented in the middle right picture can be produced. An option to keep the same number of nucleosomes as in the default case (38) but to reduce the voxel size to 64 nm, is shown in the far right picture. These modifications may be exploited to produce areas of heterochromatin and euchromatin. In the simulation, for the HTB-177 cell line, the voxel size was extended from the default value of 75 nm to 77 nm, while for the MCF-7 cells, the voxel size was reduced to 64 nm. For both these cell lines, the number of nucleosomes was kept at the constant, default "molecularDNA" value of 38. The base pair density of the HTB-177 cell is ∼0.011 bp/nm^3, while for the MCF-7 cell it is ∼0.017 bp/nm^3.

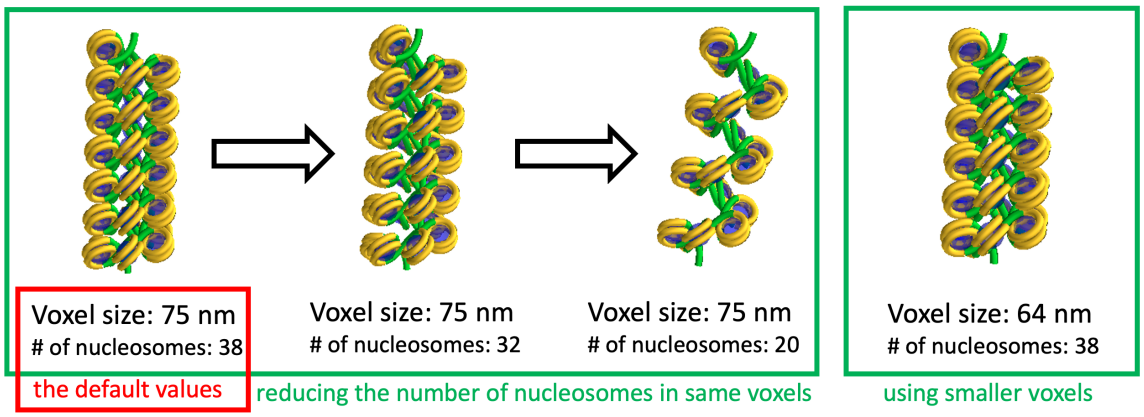

FIG. 3: The default (far left image) and modified number of nucleosomes (middle left and middle right images), as well as the voxel size that was used in this study for the MCF-7 cells (far right image).

D. Geant4 Monte Carlo simulation of alpha particle irradiation

The simulation using the "molecularDNA" example application of alpha particle irradiation of the two cancer cell lines was run in the LET range from 4 $keV/\mu m$ to 80.3 $keV/\mu m$, to match the LET range corresponding to previously published simulation results[24], and available experimental data[30] for a LET range of 4.9 $keV/\mu m$ to 40 $keV/\mu m$. The measured LET values obtained in the experimental irradiation campaign at INFN-LNS were 4.9 ± 0.1, 10.7 ± 0.3, 24.7 ± 0.4 and 39.1 ± 1.1 $keV/\mu m$[30]. Hence, in the "molecularDNA" simulation, the incident energies of alpha particles were set at the following eight values: 261, 60, 30, 20, 15, 10, 7.5, 5 MeV corresponding to the LET values of 4, 13, 22.8, 31.4, 39.2, 53.3, 65.9 and 80.3 $keV/\mu m$, respectively, according to the ICRU Report 90[45] energy to LET graph, as is shown in Figure 4. In this Figure, the orange line represents the LET to energy dependence, as provided by the ICRU Report 90 tables[45], while the blue circles correspond to the eight simulated points, spanning the targeted 4 $keV/\mu m$ to 80.3 $keV/\mu m$ range, for which data and simulation results were available.

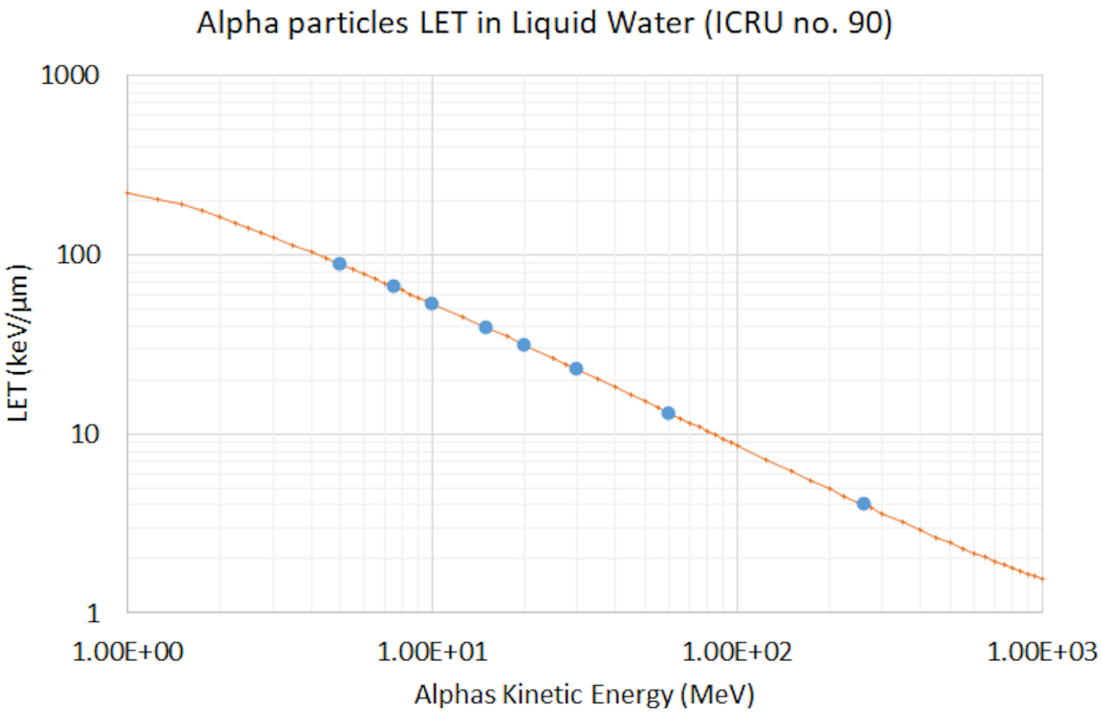

FIG. 4: The correspondence between LET and energy, as obtained from the tables in ICRU Report 90[45].

To set up the simulation, we defined several parameters[29], which have been summarized in table I. The entire cell geometry is made of liquid water and surrounded by vacuum, with the world size set to 50 μm. The distance between the source of alpha particles and the center of the targeted cell is set to 3 μm, as in Shin *et al.*[24]. The direct interaction radius was set to 2 Å. As energy threshold for inducing direct strand damage, a linear damage induction probability was set between 0 and 1 when the deposited energy goes from 5 eV to 37.5 eV, respectively. Chemistry simulation end time was set to 5 ns and the distance from the DNA geometry that chemical species are killed was set to 9 nm. Our simulations focused on the absorption by the human cell geometry of 10 Gy, to achieve an adequate statistical uncertainty.

TABLE I: Parameters used in the simulations with the "molecularDNA" example.

Parameter	Value
$R_{dir}(\mathring{A})$	2
$E_{min}^{break}(eV)$	5
$E_{max}^{break}(eV)$	37.5
p_{OH}^{break}	0.405
$T_{chem}(ns)$	5
$d_{kill}^{chem}(nm)$	9

III. RESULTS

The "molecularDNA" example application provides our estimation of the radiobiological endpoints following the particle irradiation of a human cell geometry, in terms of SSB and DSB yield and their ratio (SSB/DSB). The simulation results for the two studied human cancer cell lines are shown in Figures 5 and 6. All result values have been included in table II.

TABLE II: Simulation results using the "molecularDNA" example.

	HTB-177		MCF-7	
LET ($keV/\mu m$)	SSB/Gbp/Gy	DSB/Gbp/Gy	SSB/Gbp/Gy	DSB/Gbp/Gy
4	214 ± 15	5.4 ± 1	208 ± 14	5.2 ± 1
13	193 ± 14	6.3 ± 1	186 ± 14	6.2 ± 1
22.8	173 ± 13	7.3 ± 1	170 ± 13	7.5 ± 1
31.4	166 ± 13	8.1 ± 1	160 ± 13	8.2 ± 1
39.2	161 ± 13	9.4 ± 1	154 ± 12	9.2 ± 1
53.3	137 ± 12	10.0 ± 1	135 ± 12	10.3 ± 1
65.9	117 ± 11	10.2 ± 1	115 ± 11	10.0 ± 1
80.3	100 ± 10	11.1 ± 1	88 ± 9	10.1 ± 1

Figure 5 presents the ratio SSB/DSB as a function of LET for simulations described above for the two types of cancer cell lines, HTB-177 (green line) and MCF-7 (grey line). The studied LET goes up to 90 $keV/\mu m$, following the published simulation data of Shin *et al.*[24]. In Figure 6 the number of DSBs as a function of LET is shown, for the two cancer cell lines, in the LET range below 90 $keV/\mu m$, together with data by Shin *et al.*[24]. Experimental data by Ristic-Fira *et al.*[30] up to 40 $keV/\mu m$ are also compared with the results of these simulations.

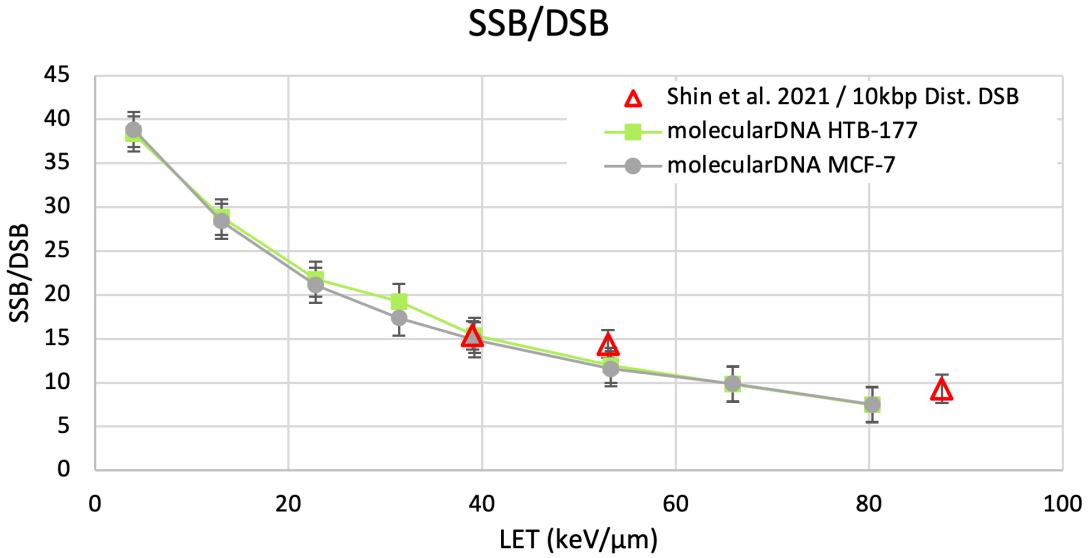

FIG. 5: The SSB/DSB ratio as a function of LET, displayed in light green and grey lines, for the HTB-177 and MCF-7 cells, respectively. The previous results of Shin *et al.*[24] are shown with red triangles.

IV. DISCUSSION

As shown in table II, the number of SSB is normalised to the dose absorbed in the nucleus and the total number of base pairs in the nucleus. Hence, the results obtained for the two cancer cell lines studied are fairly close to each other, considering their uncertainty. With the increase of LET, the number of SSB is expected to decrease. This is confirmed by the simulation made during this study, in accordance with the data provided by Shin *et al.*[24]. The comparison of the ratio SSB/DSB yield results with the same conclusions. The

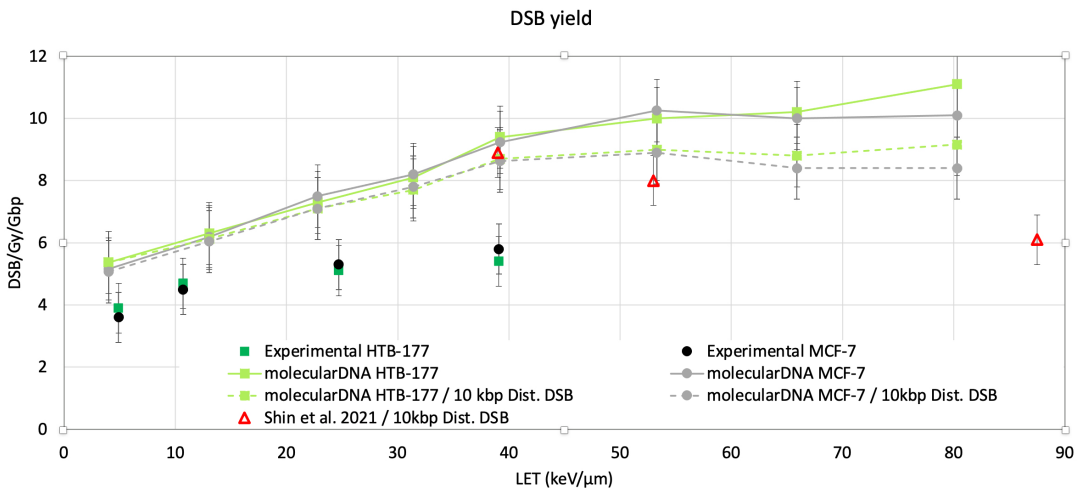

FIG. 6: The DSB yield as a function of LET, shown in light green and grey lines, for the HTB-177 and MCF-7 cells, respectively. The previous results of Shin *et al.*[24] are shown as red triangles. Experimental data[30] are shown in dark green squares and black dots, for HTB-177 and MCF-7 cell lines, respectively.

two cell lines provide very compatible results, up to the statistics applied for ∼10 Gy per simulated point. The results are compatible with earlier results by Shin *et al.*[24] and their mean difference was estimated as 10 %. It should be stated, that Shin *et al.* used a private and older version of Geant4-DNA and "molecularDNA", in comparison to this study that used the public version of "molecularDNA", which includes several differences that have been extensively discussed by Chatzipapas *et al.* [29], 2023.

In Figure 6, the number of DSBs is similarly normalised to the dose and the number of base pairs and plotted as a function of LET, which, as in the case of SSB, shows a very similar prediction for both cancer cell lines studied, and a good matching to the results of Shin *et al.*[24]. Moreover, this study used the approach established in Shin *et al.*[24], counting distant DSB that are separated by at least 10 kbp, due to limitations to detect very small DNA fragments with the experimental method used, as described in Campa *et al.*[46]. The selection of this value also allows for a direct comparison with the previously obtained MC results, as presented in Figures 5 and 6. It is also observed that for alpha particles, unlike for protons, at the LET values above 40 $keV/\mu m$ the number of DSB yield remains stable with increasing LET. This finding is consistent with the results of a previous simulation study

by Shin *et al.*[24], shown as red triangles in Figure 5, and could be explained as an overkill effect due to the lack of remaining normal DNA strands, as described in Hall and Giaccia *et al.*[47]. For the number of DSB, we consider all complex DSB to be a single DSB, including DSB++, with DSB++ as defined in Nikjoo *et al.*[48]. In terms of density of DNA in the two cell lines studied, no quantifiable difference was observed in SSB and DSB yields as well as in the ratio of SSB/DSB.

Regarding the comparison with the experimental results included in Figure 6, for both cell lines studied, the simulation results are within the experimental uncertainties, except for the highest LET of $39.1 \pm 1.1\ keV/\mu m$. The results of the "molecularDNA" simulation exceed the experimental data and this difference is more pronounced at the higher LET values that could be explained hereafter. For the detection and evaluation of DSB yields, immunofluorescent imaging of DNA repair markers such as γ-H2AX foci are used, even though the relation between foci yields and the number of DSB is not equal but proportional, and yet unclear (Ray et al. 2018[49], Sakata et al. 2020[39]). However, in experimental studies, for practical reasons, the number of foci is usually assumed to be equal to the number of DSB. It has been shown that in contrast to low-LET irradiations which produce predominantly indirect damage to DNA, high-LET irradiations are capable of directly impacting DNA molecules (Roots and Okada 1972[50], Mavragani et al. 2016[51], 2019[52]). Even though a lower irradiation dose is applied, high LET ions induce DNA lesions that are in closer proximity to one another, causing an overlapping of the fluorescent signals. Therefore, the induction of higher amounts of DSB may underestimate their number due to the limitations of the detection method which is unable to distinguish foci that are too close to each other. Moreover, clustered DNA lesions could also be the reason behind the underestimation of DSB numbers. The described behavior increases with the rise of LET, hence the values obtained by simulations are likely closer to reality than those acquired in experiments, especially for the higher values of LET.

V. CONCLUSION

This article presented one of the first validation tests of the newly released "molecularDNA" application of the Geant4-DNA package, included within the Geant4 toolkit. To perform the validation of "molecularDNA", experimental data described in Ristic-Fira *et al.*[30] were used; these data were obtained from the irradiation of the two distinct human cancer cell lines, HTB-177 and MCF-7, by helium ions.

To produce more accurate results for the two cell lines studied, new DNA geometries were developed. HTB-177 cells were measured to have a larger size than the default "human cell" model that has been included as default geometry in the "molecularDNA" application. Thus, to simulate HTB-177 cells geometry, voxels larger than the default ones were developed, as described in Section C. MCF-7 cell was measured to have a smaller size than the default "human cell", thus smaller and more dense voxels were developed for this purpose. This procedure that we have outlined in this article presented a possibility to modify the initial geometries, maintaining the human genome length at an approximate value of 6.4 Gbp[32]. This is an important stepping stone towards building a larger database of cell geometries that will become part of the Geant4-DNA package and will be available to a broader users community. Furthermore, this technique may be used to create a population of different cell types, as well as areas of heterochromatin and euchromatin.

To conclude, the simulation results presented in this work using the "molecularDNA" application showed higher yields, with up to a 30% difference at higher LET, with respect to experimental data in terms of the number of DSB for both cell lines studied. This could be attributed to the limitations of the experimental method applied, as described in IV. Discussion section. The newly created geometries for HTB-177 and MCF-7 cell lines will be made publicly available in the "molecularDNA" Geant4-DNA example. More investigation will be performed to obtain more conclusive understanding of radiation induced biological damage. These include collecting and analyzing more experimental data with different cells and in the higher LET range, as well as further simulation parameter tuning for better modeling.

VI. ACKNOWLEDGMENTS

The research was funded by the Ministry of Science, Technological Development and Innovation of the Republic of Serbia (grant number 451-03-47/2023-01/ 200017). The authors also thank the European Space Agency for its support to Geant4-DNA through the "Bio-Rad3" project (contract 4000132935/21/NL/CRS, 2021-2023). The authors wish also to acknowledge financial support obtained from CNRS through PICS "DAMOCLES" (2018-2020) and from IEA "TOLERANCE" (2023-2024) and Hubert Curien Pavle Savic (PHC) "Monte Carlo simulation of irradiation with hadron beams" (grant number 337-00-93/2023-05/18) (2023-2024) France-Serbia projects.

VII. REFERENCES

[1] I. Petrovic, A. Ristic-Fira, D. Todorovic, L. Koricanac, L. Valastro, P. Cirrone, G. Cuttone, Response of a radio-resistant human melanoma cell line along the proton spread-out Bragg peak, International Journal of Radiation Biology 86 (2010) 742–751. doi:10.3109/09553002.2010.481322.

[2] I. Petrovic, A. Ristic-Fira, O. Keta, V. Petkovic, G. Petringa, P. Cirrone, G. Cuttone, A radiobiological study of carbon ions of different linear energy transfer in resistant human malignant cell lines, International Journal of Radiation Biology 96 (2010) 1400–1412. doi:10.1080/09553002.2020.1820609.

[3] W. J. Cannan, D. S. Pederson, Mechanisms and Consequences of Double-strand DNA Break Formation in Chromatin, Journal of Cellular Physiology 231 (2016) 3–14. doi:10.1002/jcp.25048.

[4] K. Chatzipapas, P. Papadimitroulas, D. Emfietzoglou, S. Kalospyros, A. Hada, M. Georgakilas, G. Kagadis, Ionizing Radiation and Complex DNA Damage: Quantifying the Radiobiological

Damage Using Monte Carlo Simulations, Cancers 12 (2020). doi:10.3390/cancers13194940.

[5] M. Krämer, E. Scifoni, C. Schuy, M. Rovituso, W. Tinganelli, A. Maier, R. Kaderka, W. Kraft-Weyrather, S. Brons, T. Tessonnier, K. Parodi, M. Durante, Helium ions for radiotherapy? Physical and biological verifications of a novel treatment modality, Medical Physics 43 (2016) 1995–2004. doi:10.1118/1.4944593.

[6] J. S. Loeffler, M. Durante, Charged particle therapy–optimization, challenges and future directions, Nature reviews. Clinical oncology 10 (2013) 411–424. doi:10.1038/nrclinonc.2013.79.

[7] S. Mein, I. Dokic, C. Klein, T. Tessonnier, T. T. Böhlen, G. Magro, J. Bauer, A. Ferrari, K. Parodi, T. Haberer, J. Debus, A. Abdollahi, A. Mairani, Biophysical modeling and experimental validation of relative biological effectiveness (RBE) for 4He ion beam therapy, Radiation Oncology 14 (2019) 123. doi:10.1186/s13014-019-1295-z.

[8] M. Sapinski, Helium beam particle therapy facility (2020). doi:https://doi.org/10.48550/arXiv.2008.08674.

[9] W. Tinganelli, M. Durante, Carbon Ion Radiobiology, Cancers 12 (2020). doi:https://doi.org/10.3390/cancers12103022.

[10] D. K. Ebner, S. J. Frank, T. Inaniwa, S. Yamada, T. Shirai, The Emerging Potential of Multi-Ion Radiotherapy, Frontiers in Oncology 11 (2021). doi:10.3389/fonc.2021.624786.

[11] J. W. Norbury, G. Battistoni, J. Besuglow, L. Bocchini, D. Boscolo, A. Botvina, M. Clowdsley, W. de Wet, M. Durante, M. Giraudo, T. Haberer, L. Heilbronn, F. Horst, M. Krämer, C. La Tessa, F. Luoni, A. Mairani, S. Muraro, R. B. Norman, V. Patera, G. Santin, C. Schuy, L. Sihver, T. C. Slaba, N. Sobolevsky, A. Topi, U. Weber, C. M. Werneth, C. Zeitlin, Are Further Cross Section Measurements Necessary for Space Radiation Protection or Ion Therapy Applications? Helium Projectiles, Frontiers in Physics 8 (2020). doi:10.3389/fphy.2020.565954.

[12] A. Mairani, T. Tessonnier, S. Mein, D. Walsh, H. Liew, U. Weber, S. Brons, J. Debus, T. Haberer, A. Abdollahi, I. Dokic, FLASH Dose-Rate Helium Ion Beams: First In Vitro Investigations, International Journal of Radiation Oncology, Biology, Physics 111 (2021) S20–S21. doi:10.1016/j.ijrobp.2021.07.076.

[13] T. Tessonnier, S. Mein, J. Besuglow, B. Kopp, S. Ecker, J. Naumann, M. Ellerbrock, T. Held, T. Haberer, A. Debus, J. Mairani, Next Evolutions in Particle Therapy: Helium Ion Treatment Planning, Delivery and Clinical Implications of Biological Modeling, International Journal of Radiation Oncology, Biology, Physics 111 (2021) e516–e517. doi:10.1016/j.ijrobp.2021.07.

1414.

[14] A. Ottolengi, M. Merzagora, L. Tallone, M. Durante, H. Paretzke, W. Wilson, The quality of DNA double-strand breaks: A Monte Carlo simulation of the end-structure of strand breaks produced by protons and alpha particles, Radiation and Environmental Biophysics 34 (1995) 239–244. doi:10.1007/BF01209749.

[15] H. Paretzke, Radiation track structure theory. In: Freeman GR (ed) Kinetics of nonhomogeneous processes, Wiley, New York (1987) 89–1970.

[16] S. Incerti, N. Gault, C. Haabchi, J. Lefaix, P. Moretto, J. Poncy, T. Pouthier, H. Seznec, A comparison of cellular irradiation techniques with alpha particles using the Geant4 Monte Carlo simulation toolkit, Radiation Protection Dosimetry 122 (2006) 327–329. doi:10.1093/rpd/ncl422.

[17] S. Incerti, H. Seznec, M. Simon, P. Barberet, C. Habchi, P. Moretto, Monte Carlo dosimetry for targeted irradiation of individual cells using a microbeam facility, Radiation Protection Dosimetry 133 (2009) 2–11. doi:10.1093/rpd/ncp003.

[18] P. Barberet, F. Vianna, M. Karamitros, T. Brun, N. Gordillo, P. Moretto, S. Incerti, H. Seznec, Monte-Carlo dosimetry on a realistic cell monolayer geometry exposed to alpha particles, Physics in Medicine & Biology 57 (2012) 2189. doi:10.1088/0031-9155/57/8/2189.

[19] C.-Y. Huang, B. Oborn, S. Guatelli, B. Allen, Monte Carlo calculation of the maximum therapeutic gain of tumor antivascular alpha therapy, Medical Physics 39 (2012) 1282–8. doi:10.1118/1.3681010.

[20] B. Brzozowska, A. Tartas, A. Wojcik, Monte Carlo Modeling of DNA Lesions and Chromosomal Aberrations Induced by Mixed Beams of Alpha Particles and X-Rays, Frontiers in Physics 8 (2020). doi:10.3389/fphy.2020.567864.

[21] W. Friedland, P. Jacob, P. Bernhardt, et al., Simulation of DNA Damage after Proton Irradiation, Radiation Research 159 (2003) 401–410. doi:10.1667/0033-7587(2003)159[0401:SODDAP]2.0.CO;2.

[22] K. Chatzipapas, P. Papadimitroulas, M. Obeidat, K. McConnell, N. Kirby, G. Loudos, N. Papanikolaou, G. Kagadis, Quantification of DNA double-strand breaks using Geant4-DNA, Medical Physics 46 (2019) 405–413. doi:10.1002/mp.13290.

[23] K. Chatzipapas, P. Papadimitroulas, G. Loudos, N. Papanikolaou, G. Kagadis, IDDRRA: A novel platform, based on Geant4-DNA to quantify DNA damage by ionizing radiation, Medical

Physics 48 (2021) 2624–2636. doi:10.1002/mp.14817.

[24] W.-G. Shin, D. Sakata, N. Lampe, O. Belov, N. H. Tran, I. Petrovic, A. Ristic-Fira, M. Dordevic, M. A. Bernal, M.-C. Bordage, Z. Francis, I. Kyriakou, Y. Perrot, T. Sasaki, C. Villagrasa, S. Guatelli, V. Breton, D. Emfietzoglou, S. Incerti, A Geant4-DNA Evaluation of Radiation-Induced DNA Damage on a Human Fibroblast, Cancers 13 (2021). doi:10.3390/cancers13194940.

[25] E. Hoglund, E. Blomquist, J. Carlsson, B. Stenerlow, DNA damage induced by radiation of different linear energy transfer: initial fragmentation, International Journal of Radiation Biology 76 (2000) 539–547. doi:10.1080/095530000138556.

[26] S. Meylan, S. Incerti, M. Karamitros, N. Tang, M. Bueno, I. Clairand, C. Villagrasa, Simulation of early DNA damage after the irradiation of a fibroblast cell nucleus using Geant4-DNA, Scientific Reports 7 (2017). doi:10.1038/s41598-017-11851-4.

[27] N. Tang, M. Bueno, S. Meylan, S. Incerti, I. Clairand, C. Villagrasa, Simulation of early radiation-induced DNA damage on different types of cell nuclei, Radiation Protection Dosimetry 183 (2019) 26–31. doi:10.1093/rpd/ncy237.

[28] D. Frankenberg, H. Brede, U. Schrewe, C. Stenmetz, M. Frankeberg-Schwager, G. Kasten, E. Pralle, Induction of DNA double-strand breaks by 1H and 4He ions in primary human skin fibroblast in the LET range of 8 to 124 keV/um, Radiation Research 151 (1999) 540–549. doi:10.2307/3580030.

[29] K. Chatzipapas, N. H. Tran, M. Dordevic, S. Zivkovic, S. Zein, W.-G. Shin, D. Sakata, N. Lampe, J. M. Brown, A. Ristic-Fira, I. Petrovic, I. Kyriakou, D. Emfietzoglou, S. Guatelli, S. Incerti, Simulation of DNA damage using Geant4-DNA: an overview of the "molecularDNA" example application, Precision Radiation Oncology (2023). doi:10.1002/pro6.1186.

[30] A. Ristic-Fira, O. Keta, V. Petkovic, M. Dordevic, G. Petringa, S. Fattori, P. Cirrone, G. Cuttone, N. H. Tran, K. Chatzipapas, S. Incerti, I. Petrovic, Experimental Validation of Helium Ions as a Function of Linear Energy Transfer in Radioresistant Human Malignant Cells, Submitted to International Journal of Radiation Biology (2023).

[31] O. Keta, V. Petkovic, P. Cirrone, G. Petringa, G. Cuttone, D. Sakata, W.-G. Shin, S. Incerti, I. Petrovic, A. Ristic-Fira, DNA double-strand breaks in cancer cells as a function of proton linear energy transfer and its variation in time, International Journal of Radiation Biology 97 (2021) 1229–1240. doi:10.1080/09553002.2021.1948140.

[32] International Human Genome Sequencing Consortium, Finishing the euchromatic sequence of the human genome, Nature 431 (2004) 931–945. doi:10.1038/nature03001.

[33] N. Lampe, The Long Term Impact of Ionising Radiation on Living Systems, Ph.D. thesis, Université Clermont Auvergne, Clermont, France, 2017.

[34] N. Lampe, M. Karamitros, V. Breton, J. M. Brown, I. Kyriakou, D. Sakata, D. Sarramia, S. Incerti, Mechanistic DNA damage simulations in Geant4-DNA part 1: A parameter study in a simplified geometry, Physica Medica: European Journal of Medical Physics 48 (2018) 135–147. doi:10.1016/j.ejmp.2018.02.011.

[35] N. Lampe, M. Karamitros, V. Breton, J. M. Brown, I. Kyriakou, D. Sakata, D. Sarramia, S. Incerti, Mechanistic DNA damage simulations in Geant4-DNA part 2: Electron and proton damage in a bacterial cell, Physica Medica: European Journal of Medical Physics 48 (2018) 146–155. doi:10.1016/j.ejmp.2017.12.008.

[36] N. Lampe, 2021, FractalDNA. GitHub, https://github.com/natl/fractaldna.

[37] D. Sakata, R. Hirayama, W.-G. Shin, M. Belli, M. A. Tabocchini, R. D. Stewart, O. Belov, M. A. Bernal, M.-C. Bordage, J. M. Brown, M. Dordevic, D. Emfietzoglou, Z. Francis, S. Guatelli, T. Inaniwa, V. Ivanchenko, M. Karamitros, I. Kyriakou, N. Lampe, Z. Li, S. Meylan, C. Michelet, P. Nieminen, Y. Perrot, I. Petrovic, J. Ramos-Mendez, A. Ristic-Fira, G. Santin, J. Schuemann, H. N. Tran, C. Villagrasa, S. Incerti, Prediction of DNA rejoining kinetics and cell survival after proton irradiation for V79 cells using Geant4-DNA, Physica Medica: European Journal of Medical Physics 105 (2022). doi:10.1016/j.ejmp.2022.11.012.

[38] D. Sakata, M. Suzuki, R. Hirayama, Y. Abe, M. Muramatsu, S. Sato, O. Belov, I. Kyriakou, D. Emfietzoglou, S. Guatelli, S. Incerti, T. Inaniwa, Performance Evaluation for Repair of HSGc-C5 Carcinoma Cell Using Geant4-DNA, Cancers 13 (2021). doi:10.3390/cancers13236046.

[39] D. Sakata, O. Belov, M.-C. Bordage, D. Emfietzoglou, S. Guatelli, T. Inaniwa, V. Ivanchenko, M. Karamitros, I. Kyriakou, N. Lampe, I. Petrovic, A. Ristic-Fira, W.-G. Shin, S. Incerti, Fully integrated Monte Carlo simulation for evaluating radiation induced DNA damage and subsequent repair using Geant4-DNA, Scientific Reports 10 (2020). doi:10.1038/s41598-020-75982-x.

[40] D. Sakata, N. Lampe, M. Karamitros, I. Kyriakou, O. Belov, M. A. Bernal, D. Bolst, M.-C. Bordage, V. Breton, J. M. Brown, Z. Francis, V. Ivanchenko, S. Meylan, K. Murakami, S. Okada, I. Petrovic, A. Ristic-Fira, G. Santin, D. Sarramia, T. Sasaki, W.-G. Shin, N. Tang,

H. N. Tran, C. Villagrasa, D. Emfietzoglou, P. Nieminen, S. Guatelli, S. Incerti, Evaluation of early radiation DNA damage in a fractal cell nucleus model using Geant4-DNA, Physica Medica: European Journal of Medical Physics 62 (2019) 152–157. doi:10.1016/j.ejmp.2019.04.010.

[41] W.-G. Shin, J. Ramos-Mendez, N. H. Tran, S. Okada, Y. Perrot, C. Villagrasa, S. Incerti, Geant4-DNA simulation of the pre-chemical stage of water radiolysis and its impact on initial radiochemical yields, Physica Medica: European Journal of Medical Physics 88 (2021) 86–90. doi:10.1016/j.ejmp.2021.05.029.

[42] F. Chappuis, V. Grilj, H. Ngoc Tran, S. A. Zain, F. Bochud, C. Bailat, S. Incerti, L. Desorger, Modeling of scavenging systems in water radiolysis with Geant4-DNA, Physica Medica: European Journal of Medical Physics 108 (2023). doi:10.1016/j.ejmp.2023.102549.

[43] M. Pietrzak, H. Nettelbeck, Y. Perrot, C. Villagrasa, A. Bancer, M. Bug, S. Incerti, Intercomparison of nanodosimetric distributions in nitrogen simulated with Geant4 and PTra track structure codes, Physica Medica: European Journal of Medical Physics 102 (2022) 103–109. doi:110.1016/j.ejmp.2022.09.003.

[44] W. Rasband, 1997-2018, ImageJ. U. S. National Institutes of Health, Bethesda, Maryland, USA, https://imagej.nih.gov/ij/.

[45] 2016, ICRU Report 90, Key Data For Ionizing-Radiation Dosimetry. https://www.icru.org/report/icru-report-90-key-data-for-ionizing/-radiation-dosimetry-measurement-standards-and-applications/.

[46] A. Campa, F. Ballarini, M. Belli, R. Cherubini, V. Dini, G. Esposito, W. Friedland, S. Gerardi, S. Molinelli, A. Ottolenghi, H. Paretzke, G. Simone, M. A. Tabocchini, DNA DSB induced in human cells by charged particles and gamma rays: experimental results and theoretical approaches, International Journal of Radiation Biology 81 (2005) 841–54. doi:10.1080/09553000500530888.

[47] E. Hall, A. J. Giaccia, 2018, Radiobiology for Radiologist. Lippincott Williams and Wilkins.

[48] H. Nikjoo, P. O'Neill, D. T. Goodhead, M. Terrissol, Computational modelling of low-energy electron-induced DNA damage by early physical and chemical events, International Journal of Radiation Biology 71 (1997) 467–483. doi:10.1080/095530097143798.

[49] S. Ray, E. Cekanaviciute, I. Lima, B. Sorensen, S. Costes, PComparing photon and charged particle therapy using DNA damage biomarkers, International Journal of Particle Therapy 5 (2018) 15–24. doi:10.14338/IJPT-18-00018.1.

[50] R. Roots, S. Okada, Protection of DNA molecules of cultured mammalian cells from radiation-

induced single-strand scissions by various alcohols and SH compounds, International Journal of Radiation Biology and Related Studies in Physics, Chemistry and Medicine 21 (1972) 329–342. doi:10.1080/09553007214550401.

[51] I. Mavragani, D. Laskaratou, B. Frey, S. Candéias, U. Gaipl, K. Lumniczky, A. Georgakilas, Key mechanisms involved in ionizing radiation-induced systemic effects. A current review., Toxicology Research 5 (2016) 12–33. doi:10.1039/C5TX00222B.

[52] I. Mavragani, Z. Nikitaki, S. A. Kalospyros, A. G. Georgakilas, Ionizing Radiation and Complex DNA Damage: From Prediction to Detection Challenges and Biological Significance, Cancers 11 (2019). doi:10.3390/cancers11111789.